

ՀՀ ԿՐԹՈՒԹՅԱՆ ԵՎ ԳԻՏՈՒԹՅԱՆ ՆԱԽԱՐԱՐՈՒԹՅՈՒՆ
ԵՐԵՎԱՆԻ ՊԵՏԱԿԱՆ ՀԱՄԱԼՍԱՐԱՆ

ՍԱՀԱՐՅԱՆ ՆՎԱՐԴ ԱՐԱՄԻ

ՈՐՈՇ ՔՎԱՆՏԱՅԻՆ ԵՐԵՎՈՒՅԹՆԵՐ ԳՐԱՎԻՏԱՑԻՈՆ ԴԱՇՏԵՐՈՒՄ

Ա.04.02 - <<Տեսական ֆիզիկա>> մասնագիտությամբ
ֆիզիկամաթեմատիկական գիտությունների թեկնածուի
գիտական աստիճանի հայցման ատենախոսության

ՍԵՂՄԱԳԻՐ

ԵՐԵՎԱՆ - 2019

MINISTRY OF EDUCATION AND SCIENCE OF THE REPUBLIC OF ARMENIA
YEREVAN STATE UNIVERSITY

SAHARYAN NVARD ARAMI

SOME QUANTUM PHENOMENA IN GRAVITATIONAL FIELDS

Thesis for the degree of Candidate of physical and mathematical sciences
Speciality 01.04.02 - "Theoretical Physics"

ABSTRACT

YEREVAN - 2019

Ատենախոսության թեման հաստատվել է Երևանի պետական համալսարանում

Գիտական ղեկավար՝
Պաշտոնական
ընդդիմախոսներ՝

Ֆիզ.-մաթ. գիտ. դոկտոր, պրոֆեսոր Ռ.Մ. Ավագյան
Ֆիզ.-մաթ. գիտ. դոկտոր, պրոֆեսոր
Ֆիզ.-մաթ. գիտ. դոկտոր, պրոֆեսոր

Առաջատար
կազմակերպություն՝

Ատենախոսության պաշտպանությունը կայանալու է 2019թ. Երևանի պետական համալսարանում գործող Ֆիզիկայի 049 Մասնագիտական խորհրդի նիստում

Հասցե՝ 0025 Երևան, Ալեք Մանուկյան փ. 1, ԵՊՀ

Ատենախոսությանը կարելի է ծանոթանալ ԵՊՀ գրադարանում:

Սեղմագիրն առաքված է 2019թ.

Մասնագիտական խորհրդի
գիտական քարտուղար՝

Ֆիզ.-մաթ. գիտ. թեկնածու
Վ.Պ. Քալանթարյան

The thesis theme is confirmed at the Yerevan State University

Scientific supervisor:
Official opponents:

Doctor of Phys. Math. Sciences Prof. R.M. Avagyan
Doctor of Phys. Math. Sciences, Prof.
Doctor of Phys. Math. Sciences, Prof.

Leading organization:

The defense of the thesis will take place on the session of the Specialized Council 049 Physics of the Yerevan State University

Address: 1 Alex Manoogian Street, 0025 Yerevan, Armenia

The thesis is available in the library of the Yerevan State University

The abstract is distributed on

Scientific secretary of
the Specialized Council

Candidate of Phys. Math. Sciences
V.P. Kalantaryan

GENERAL DESCRIPTION OF THE WORK

Relevance of topic. The properties of vacuum fluctuations of quantum fields depend on external fields and on the geometry of the background spacetime. Among the most interesting effects of this kind is the dependence of the properties of the vacuum on boundary conditions imposed on a quantum field. The boundary conditions modify the spectrum of vacuum fluctuations and, as a result of that, the vacuum expectation values (VEVs) of physical observables are changed. The change in the vacuum properties induced by boundary conditions is called the Casimir effect. Currently it has been investigated in large number of the bulk and boundary geometries (see [1,2]). The Casimir effect can be considered as a consequence of the vacuum polarization by boundaries. Another kind of vacuum polarization arises in an external gravitational field. An interesting topic in the theory of the Casimir effect is the investigation of the dependence of the local characteristics, like the energy density and stresses, on the background gravitational field. In the corresponding calculations the knowledge of a complete set of the field modes is required and exact results can be obtained for bulk and boundary geometries having high degree of symmetry.

The investigation of quantum effects in curved backgrounds is motivated by several reasons. During the cosmological expansion of the Universe, the back reaction of the particles created by a time dependent gravitational field at early stages leads to a rapid isotropization of the expansion. According to the inflationary scenario, the quantum vacuum fluctuations of a scalar field, amplified by the gravitational field during the quasi-de Sitter (dS) like expansion, serve as seeds for the large scale structure formation in the Universe. The information on the properties of these fluctuations are encoded in the thermal anisotropies of the cosmic microwave background which are measured with high accuracy by a number of recent cosmological projects. An important feature of quantum field theory in curved backgrounds is a possible breakdown of the energy conditions in the formulations of Hawking-Penrose singularity theorems, by the expectation value of the energy-momentum tensor of quantum fields. This opens a possibility to solve the singularity problem within the framework of classical general relativity. An additional motivation for the study of quantum field theoretical effects in curved backgrounds appeared recently in condensed matter physics related to various analog models. In particular, the long wavelength properties of the electronic subsystem in a graphene sheet are well described by the Dirac-like model with the speed of light replaced by the Fermi velocity. In curved graphene structures (for example, in fullerenes) the corresponding field theory is formulated on curved geometry and the curvature effects should be taken into account in the calculations of physical properties of these structures [3,4].

The boundary conditions on the field operator can also be induced by nontrivial topology of the space. The changes in the properties of the vacuum state generated by this type of conditions are referred to as the topological Casimir effect. The importance of this effect is motivated by that the presence of compact dimensions is an inherent feature in many high-energy theories of fundamental physics, in cosmology and in condensed matter physics. In particular, supergravity and superstring theories are formulated in spacetimes having extra compact dimensions. The compactified higher-dimensional models provide a possibility for the unification of known interactions. Models of a compact universe with nontrivial topology may also play an important role by providing proper initial conditions for inflation in the early stages of the Universe expansion. In condensed matter physics, a number of planar systems in the low-energy sector are described by an effective field theory. The compactification of these systems leads to the change in the ground state energy which is the analog of the topological Casimir

effect. Well-known examples of this type are cylindrical and toroidal carbon nanotubes, having topologies $R^1 \times S^1$ and T^2 (2-dimensional torus), respectively. These structures are generated by rolling up a graphene sheet.

The aim of the thesis is the investigation of combined effects of constraining boundaries, background geometry and nontrivial topology on the local properties of the vacuum state for scalar and electromagnetic fields. We have studied:

- Wightman function, the VEVs of the field squared and of the energy-momentum tensor for a quantum scalar field on the background of a negatively curved constant curvature space in the presence of a spherical boundary with Robin boundary condition on it,
- Effect of two parallel plane boundaries on the VEV of the current density for a charged scalar field in flat spacetime with toroidally compactified spatial dimensions,
- Electromagnetic field modes, the VEVs of the electric and magnetic fields squared and of the energy-momentum tensor inside and outside a cylindrical shell in dS spacetime,
- Influence of a cosmic string on the vacuum fluctuations of the electromagnetic field in background of dS spacetime.

Scientific novelty. The Wightman function, the mean field squared and the VEV of the energy-momentum tensor are evaluated for a scalar field with Robin boundary condition on a spherical shell in the background of a constant negative curvature space. For the coefficient in the boundary condition there is a critical value above which the scalar vacuum becomes unstable. At distances from the sphere larger than the curvature scale of the background space the suppression of the vacuum fluctuations in the gravitational field corresponding to the negative curvature space is stronger compared with the case of the Minkowskian bulk. The Hadamard function and the VEV of the current density are investigated for a charged scalar field in the geometry of flat boundaries with an arbitrary number of toroidally compactified spatial dimensions and in the presence of a constant gauge field. The latter induces Aharonov-Bohm-type effect on the VEVs. The vacuum stability condition depends on the lengths of compact dimensions and is less restrictive than that for background with trivial topology. Complete set of cylindrical modes is constructed for the electromagnetic field inside and outside a cylindrical shell in the background of dS spacetime and the VEVs of the electric field squared and of the energy-momentum tensor are evaluated. The vacuum energy-momentum tensor has a nonzero off-diagonal component that corresponds to the energy flux. For a cosmic string in dS spacetime, the electromagnetic field correlators are presented in the form with explicitly separated topological parts. Near the string the VEVs are dominated by the topological contributions and the effects induced by the gravitational field are small. At distances from the string larger than the curvature radius of the background geometry, the pure dS parts in the VEVs dominate.

Practical importance. The methods used in the thesis can be used for the investigation of the VEVs of local physical observables for other geometries of background spacetime. In particular, they include spaces with spherical bubbles and for cosmological models with negative curvature spaces. The expressions for the two-point functions can be used for the study of the response of Unruh-de Witt type particle detectors in a given state of motion. The generalized Abel-Plana-type summation formula for series over the zeros of the linear combination of the associated Legendre function and its derivative can be used in other problems of mathematical physics on background of negatively curved space.

Basic results to be defended:

1. For a scalar field with Robin boundary condition on a spherical shell in the background of a constant negative curvature the boundary-induced parts are explicitly extracted from the VEVs of the field squared and of the energy-momentum tensor. At large distances from the sphere the decay of those parts is stronger compared with the case of a sphere in Minkowski bulk. Depending on the coefficient in the boundary condition, the vacuum energy density can be either positive or negative.
2. In spacetimes with toroidally compactified spatial dimensions, the nontrivial phases in quasiperiodicity conditions for a charged scalar field and a constant gauge field induce vacuum currents along compact dimensions. The current density is a periodic function of the magnetic flux, enclosed by compact dimensions, with the period equal to the flux quantum. Depending on the boundary conditions, the presence of planar boundaries may decrease or increase the VEV of the current density.
3. In both the problems with spherical and planar boundaries, there is a region in the space of the parameters in Robin boundary conditions where the vacuum state is unstable. The stability condition depends on the background geometry and topology.
4. For a cylindrical shell in dS spacetime, the boundary-induced contribution in the VEV of the electric field squared is positive for both the interior and exterior regions and the corresponding Casimir-Polder forces are directed toward the shell. The vacuum energy density, as a function of the distance from the shell, may change the sign. The presence of the cylindrical shell induces an energy flux directed from the shell.
5. For the electromagnetic field around a cosmic string in dS spacetime, the topological contributions in the local characteristics of the vacuum are explicitly separated. At distances from the string smaller than the dS curvature radius the influence of the gravitational field is weak and those contributions dominate in the VEVs. At larger distances from the string the effect of the gravity is essential and the behavior of the VEVs may crucially differ from that for a string in Minkowski bulk. Depending on the planar angle deficit induced by the string, the vacuum energy density can be either positive or negative.

Approbation of the work. The results of the thesis were reported at the conferences "Modern Physics of Compact Stars and Relativistic Gravity" (Yerevan, 2017), "Casimir Effect: Theory and Applications" (Trondheim, Norway, 2018), "Verao Quantico 2019" (Ubu-Anchieta, Brazil, 2019) and have been discussed at the seminars of the Chair of theoretical physics of Yerevan State University, of the INFN National Laboratory of Frascati (Frascati, Italy) and of the Federal University of Paraiba (Joao Pessoa, Brazil).

Publications. Seven papers are published on the topic of the thesis.

Structure of the thesis. The thesis consists of Introduction, four Chapters, Conclusion and the list of references. It contains 159 pages, including 11 figures.

CONTENT OF THE THESIS

In **Introduction** the scientific literature related to the topic of the thesis is reviewed, the relevance of the topic is argued, the aim of the work, the scientific novelty and the practical value are presented, the basic results to be defended are given.

In Chapter 1 the influence of background gravitational field and of a spherical shell on local properties of the vacuum for a scalar field is investigated. The field dynamics is described by the Klein-Gordon equation

$$(\nabla_l \nabla^l + m^2 + \xi \mathcal{R})\varphi(x) = 0, \quad (1)$$

where \mathcal{R} is the Ricci scalar, ∇_l is the covariant derivative operator, ξ is the curvature coupling parameter. The background geometry is described by the line element

$$ds^2 = dt^2 - a^2(dr^2 + \sinh^2 r d\Omega_{D-1}^2), \quad (2)$$

with a constant a and with $d\Omega_{D-1}^2$ being the line element on the $(D - 1)$ -dimensional sphere with unit radius, S^{D-1} . The spatial part of the line element (2) describes a constant negative curvature space. The spaces with negative curvature play a significant role in cosmology and in holographic theories. As a boundary geometry we consider a spherical shell with radius $r = r_0$ on which the field operator obeys Robin boundary condition

$$(A + B n^l \nabla_l) \varphi(x) = 0, \quad (3)$$

where A and B are constants, and n^l is the unit inward normal to the sphere, $n^l = -\delta_{(j)}^l / a$, $j = i, e$, with $\delta_{(i)} = 1$ for the interior region and $\delta_{(e)} = -1$ for the exterior region.

For a free field theory all the properties of the quantum vacuum are contained in two-point functions. As such the positive-frequency Wightman function is considered, defined as the VEV $W(x, x') = \langle 0 | \varphi(x) \varphi(x') | 0 \rangle$, where $|0\rangle$ corresponds to the vacuum state. The expectation values of physical characteristics bilinear in the field operator are obtained from this function in the coincidence limit. In addition to this, the positive-frequency Wightman function determines the response function for the Unruh-De Witt particle detector in a given state of motion. In order to evaluate the Wightman function we employ the direct summation over the complete set of modes. In the region inside the sphere, the eigenmodes of the field are expressed in terms of the zeros of the combination of the associated Legendre function and its derivative with respect to the order. In the mode-sum for the Wightman function, for the summation of the series over these zeros we apply the formula, derived from the generalized Abel-Plana formula. This allowed to separate the part corresponding to the boundary-free geometry and to present the sphere-induced part in terms of a rapidly convergent integral. In that form the explicit knowledge of the eigenmodes is not required. In addition, with the decomposition into the boundary-free and boundary-induced contributions, the renormalization of the VEVs in the coincidence limit is reduced to the one for the boundary-free geometry. A similar decomposition for the exterior region, $r > r_0$, is provided.

In Section 1.2, as an important local characteristic of the vacuum state, the VEV of the field squared is considered. It is decomposed as $\langle \varphi^2 \rangle = \langle \varphi^2 \rangle_0 + \langle \varphi^2 \rangle_s$, where $\langle \varphi^2 \rangle_0$ is the renormalized VEV in the boundary-free space and the part $\langle \varphi^2 \rangle_s$ is induced by the sphere. In the region inside the sphere, $r < r_0$, the latter is given by

$$\langle \varphi^2 \rangle_s = -\frac{a^{1-D}}{\pi S_D} \sum_{l=0}^{\infty} D_l e^{-i\mu\pi} \int_{z_m}^{\infty} dz z \frac{\bar{Q}_{z-1/2}^{\mu}(\cosh r_0)}{\bar{P}_{z-1/2}^{-\mu}(\cosh r_0)} \frac{[P_{z-1/2}^{-\mu}(\cosh r)]^2}{\sinh^{D-2} r \sqrt{z^2 - z_m^2}}, \quad (4)$$

where $S_D = 2\pi^{D/2}/\Gamma(D/2)$ is the surface area of the unit sphere in D -dimensional space, $P_{z-1/2}^{-\mu}(u)$ and $Q_{z-1/2}^{\mu}(u)$ are the associated Legendre functions,

$$\mu = l + D/2 - 1, \quad D_l = 2\mu \frac{\Gamma(l + D - 2)}{\Gamma(D - 1)l!}, \quad z_m = \sqrt{m^2 a^2 - D(D - 1)(\xi - \xi_c)}, \quad (5)$$

$\xi_c = (D-1)/(4D)$ is the curvature coupling parameter for a conformally coupled field. Here, for a given function $F(u)$ we use the notation $\bar{F}(u) = A(u)F(u) + B(u)F'(u)$, with the coefficients

$$A(u) = A\sqrt{u^2 - 1} + (D/2 - 1)\delta_{(j)}\frac{B}{a}u, \quad B(u) = -\delta_{(j)}\frac{B}{a}(u^2 - 1). \quad (6)$$

The expressions for the sphere-induced part in the exterior region ($r > r_0$) is obtained from (4) by the replacements $P \rightleftharpoons Q$ of the associated Legendre functions. For both the interior and exterior regions the sphere-induced VEV of the field squared is negative for Dirichlet boundary condition ($B = 0$) and positive for Neumann boundary condition ($A = 0$). The expectation value of the field squared diverges on the boundary. The leading term in the asymptotic expansion over the distance from the sphere behaves as $1/|r_0 - r|^{D-1}$ and coincides with that for the sphere in Minkowski bulk. This is natural, because near the sphere the contribution of the modes with the wavelengths smaller than the curvature radius dominate and they are relatively insensitive to the background geometry. In the opposite limit of large distances, the effects of gravity are decisive and the VEV decays as $\langle \varphi^2 \rangle_s \propto e^{-(2z_m + D-1)r}$. For both massive and massless fields the suppression of the boundary-induced VEV at large distances is exponential. This is in contrast to the case of Minkowskian bulk, where the decay for massless fields has a power-law behavior.

In Section 1.3 the VEV of the energy-momentum tensor is investigated. It is presented in decomposed form $\langle T_{ik} \rangle = \langle T_{ik} \rangle_0 + \langle T_{ik} \rangle_s$, where the first and second terms in the right-hand side correspond to the boundary-free and sphere-induced contributions. The vacuum energy-momentum tensor is diagonal and the expressions for the sphere-induced contributions inside the sphere are given by (no summation over k)

$$\langle T_k^k \rangle_s = \frac{a^{-1-D}}{\pi S_D} \sum_{l=0}^{\infty} D_l e^{-i\mu\pi} \int_{z_m}^{\infty} dz z \frac{\bar{Q}_{z-1/2}^{\mu}(\cosh r_0) F^{(k)}[P_{z-1/2}^{-\mu}(\cosh r)]}{\bar{P}_{z-1/2}^{-\mu}(\cosh r_0) \sinh^{D-2} r \sqrt{z^2 - z_m^2}}, \quad (7)$$

where $F^{(k)}[f(x)]$, $k = 0, 1, \dots, D$, are bilinear functions of $f(x)$ and its derivative $f'(x)$. The VEV outside the sphere is obtained with the replacements $P \rightleftharpoons Q$ in the integrand of (7). The part in the VEV of the energy-momentum tensor induced by the spherical shell satisfies the covariant conservation equation $\nabla_k \langle T_i^k \rangle_s = 0$. Near the sphere, the leading term in the energy density and parallel stresses is given by (no summation over k)

$$\langle T_k^k \rangle_s \approx \frac{D\Gamma((D+1)/2)(\xi - \xi_c)(2\delta_{0B} - 1)}{2^D \pi^{(D+1)/2} (a|r_0 - r|)^{D+1}}, \quad (8)$$

for the components $k = 0, 2, \dots$. These leading terms coincide with those for a sphere in the Minkowski bulk. For the leading term of the radial stress one has

$$\langle T_1^1 \rangle_s \approx (1 - 1/D) (r_0 - r) \coth r_0 \langle T_0^0 \rangle_s, \quad (9)$$

and the corresponding divergence is weaker. At large distances from the sphere the VEVs are suppressed by the factor $e^{-(2z_m + D-1)r}$. Again, in contrast to the Minkowskian case, the expectation values are exponentially suppressed for both massive and massless fields.

In Section 1.4 we generalize the results for the VEVs to the backgrounds described by two distinct spherically symmetric metric tensors in the regions separated by a spherical boundary. The geometry of one region affects the properties of the vacuum in the other region leading to the gravitationally induced Casimir effect. We have considered the interior geometry ($r < r_0$, bubble) described by the line element

$$ds^2 = e^{2u(r)} dt^2 - a^2 [e^{2v(r)} dr^2 + e^{2w(r)} d\Omega_{D-1}^2], \quad (10)$$

with general functions $u(r)$, $v(r)$, $w(r)$, and the geometry in the region $r > r_0$ is given by (2). For generality, the presence of the surface energy-momentum tensor with nonzero components τ_0^0 and $\tau_2^2 = \dots = \tau_D^D$, located at $r = r_0$, is assumed. The continuity of the metric tensor at the separating boundary implies $u(r_0) = v(r_0) = 0$, $w(r_0) = \ln(\sinh r_0)$. From the Israel matching conditions on the sphere $r = r_0$ the components of the surface energy-momentum tensor τ_i^k are expressed in terms of $u'(r_0)$ and $w'(r_0)$. The boundary conditions for the field operator on the sphere $r = r_0$ are obtained from the field equation. In the region $r > r_0$, the bubble-induced contributions in the Wightman function and in the VEVs of the field squared and the energy-momentum tensor are obtained from the expressions for the spherical shell with Robin boundary condition by the replacement

$$\frac{aA}{B} \rightarrow -\frac{R'_{(i)l}(r_0, e^{\pi i/2} \sqrt{z^2 - z_m^2})}{R_{(i)l}(r_0, e^{\pi i/2} \sqrt{z^2 - z_m^2})} - 2\xi \{u'(r_0) + (D-1)[w'(r_0) - \coth r_0]\}, \quad (11)$$

where $R_{(i)l}(r, E)$ is the real solution of the field equation for the radial function in the interior region, regular at the bubble center, and E is the corresponding energy. As an example of the interior geometry we have considered the case of the Minkowskian bubble. In the geometry with bubbles the divergences on the boundary are weaker compared with the case of the Robin sphere. We have also considered a bubble with a negative constant curvature space in the Minkowski bulk.

The generalization of the results for the Friedmann-Robertson-Walker cosmological models with a time-dependent scale factor is straightforward in the case of a conformally coupled massless field. This requires the replacement $a \rightarrow a(t)$ in the expressions for the Wightman function and for the vacuum expectation values. In the special case $D = 2$, the results obtained can be applied to negatively curved graphene structures, described in the long-wavelength regime by an effective 3-dimensional relativistic field theory. The latter, in addition to the well-known Dirac fermions describing the low-energy excitations of the electronic subsystem, involves scalar and gauge fields originating from the elastic properties and describing disorder phenomena, like the distortions of the graphene lattice and structural defects (see, for example, [5,6]). In this setup, the spherical boundary models the edge of a negatively curved graphene sheet. The boundary condition we have used ensures the zero flux of a scalar field through the boundary.

In Chapter 2 the influence of parallel flat boundaries on the VEV of the current density is investigated for a charged scalar field $\varphi(x)$ in a flat spacetime with spatial topology $R^{p+1} \times T^q$, $p+q+1 = D$, where T^q stands for a q -dimensional torus. In addition, the presence of an abelian gauge field A_μ is assumed. The set of Cartesian coordinates in the subspace R^{p+1} will be denoted by $\mathbf{x}_{p+1} = (x^1, \dots, x^{p+1})$ and the corresponding coordinates on the torus by $\mathbf{x}_q = (x^{p+2}, \dots, x^D)$. If L_l is the length of the l th compact dimension then one has $-\infty < x^l < \infty$ for $l = 1, \dots, p$, and $0 \leq x^l \leq L_l$ for $l = p+2, \dots, D$. The field equation has the form (1), where now $\nabla_\mu = \partial_\mu + ieA_\mu$, with e being the charge of the field quanta, and $\mathcal{R} = 0$. We assume the presence of two parallel flat boundaries placed at $x^{p+1} = a_1$ and $x^{p+1} = a_2$. On the boundaries the field obeys Robin boundary conditions (compare with (3))

$$(1 + \beta_j n_j^\mu \nabla_\mu) \varphi(x) = 0, \quad x^{p+1} \equiv z = a_j, \quad (12)$$

with constant coefficients β_j , $j = 1, 2$, and with n_j^μ being the inward pointing normal to the boundary at $x^{p+1} = a_j$. Here, for the further convenience we have introduced a special notation $z = x^{p+1}$ for the $(p+1)$ th spatial dimension. In the region between the plates, $a_1 \leq z \leq a_2$,

one has $n_j^\mu = (-1)^{j-1} \delta_{p+1}^\mu$. The expressions for the VEVs in the regions $z \leq a_1$ and $z \geq a_2$ are obtained by the limiting transitions. In addition to the boundary conditions on the plates, for the theory to be completely defined, one needs to specify the periodicity conditions along the compact dimensions. Different conditions correspond to topologically inequivalent field configurations. We consider generic quasiperiodicity conditions,

$$\varphi(t, x^1, \dots, x^l + L_l, \dots, x^D) = e^{i\alpha_l} \varphi(t, x^1, \dots, x^l, \dots, x^D), \quad (13)$$

with constant phases α_l , $l = p+2, \dots, D$. The special cases of (13) with $\alpha_l = 0$ and $\alpha_l = \pi$ correspond to the most frequently discussed cases of untwisted and twisted scalar fields.

The VEV of the current density is obtained from the Hadamard two-point function $G(x, x')$ by using the formula

$$\langle 0 | j_\mu(x) | 0 \rangle \equiv \langle j_\mu(x) \rangle = \frac{i}{2} e \lim_{x' \rightarrow x} (\partial_\mu - \partial'_\mu + 2ieA_\mu) G(x, x'). \quad (14)$$

The Hadamard function is evaluated by mode-sum formula that contains the summation over the complete set of scalar modes. In the region between the plates, the eigenvalues of the momentum component normal to the plates are given as roots of transcendental equation. By using the generalized Abel-Plana formula for summation of the series over those roots, the Hadamard function is decomposed into boundary-free, single boundary-induced and the second boundary-induced contributions. In the case $1/\beta_j > \omega_0$, where $\omega_0^2 = \sum_{l=p+2}^D \tilde{\alpha}_l^2 / L_l^2 + m^2$ and $\tilde{\alpha}_l = \alpha_l + eA_l L_l$, there are scalar field modes for which the energy is imaginary and the vacuum is unstable. In order to have a stable vacuum, for non-Dirichlet boundary conditions, it is assumed that $1/\beta_j < \omega_0$. The physical quantities are periodic functions of $\tilde{\alpha}_l$ with the period 2π and in the definition of ω_0 we assume that $|\tilde{\alpha}_l| \leq \pi$. The momentum k_l along the l th compact dimension is quantized by the condition (13) and $k_l = (2\pi n_l + \tilde{\alpha}_l) / L_l$, with $n_l = 0, \pm 1, \pm 2, \dots$. The current density in the boundary-free geometry has been investigated in [7]. The corresponding charge density and the current densities along uncompact dimensions vanish. The same holds in the case of the boundary-induced contributions in the VEVs. Hence, the only nonzero components correspond to the current density along compact dimensions. The latter is a periodic function of the magnetic flux with the period equal to the flux quantum. The component along the l th compact dimension is an odd function of the phase $\tilde{\alpha}_l$ and an even function of the remaining phases $\tilde{\alpha}_i$, $i \neq l$.

In Section 2.2 we investigate the VEV of the vacuum current density in the geometry of a single plate at $x^{p+1} = a_j$. This VEV is obtained with the help of the formula (14) by using the corresponding Hadamard function. The component of the VEV of the current density along the l th compact dimension is presented in the decomposed form $\langle j^l \rangle_j = \langle j^l \rangle_0 + \langle j^l \rangle_j^{(1)}$, where $\langle j^l \rangle_0$ is the current density in the boundary-free geometry and $\langle j^l \rangle_j^{(1)}$ is the contribution induced by the presence of the plate. For the latter one gets

$$\langle j^l \rangle_j^{(1)} = \frac{e\pi^{-(p+1)/2}}{2^p \Gamma((p+1)/2) V_q} \sum_{\mathbf{n}_q} k_l \int_{\omega_{\mathbf{n}_q}}^\infty dy (y^2 - \omega_{\mathbf{n}_q}^2)^{(p-1)/2} e^{-2yz_j} \frac{y\beta_j + 1}{y\beta_j - 1}, \quad (15)$$

where $V_q = L_{p+1} \dots L_D$ is the volume of the compact subspace, $z_j = |z - a_j|$ is the distance from the plate, $\mathbf{n}_q = (n_{p+2}, \dots, n_D)$, and $\omega_{\mathbf{n}_q}^2 = \sum_{l=p+2}^D k_l^2 + m^2$. In the special cases of Dirichlet and Neumann boundary conditions we obtain

$$\langle j^l \rangle_j^{(1)} = \mp \frac{2e/V_q}{(2\pi)^{p/2+1}} \sum_{\mathbf{n}_q} k_l \omega_{\mathbf{n}_q}^p f_{p/2}(2\omega_{\mathbf{n}_q} z_j), \quad f_\nu(x) \equiv \frac{K_\nu(x)}{x^\nu}, \quad (16)$$

where the upper and lower signs correspond to Dirichlet and Neumann boundary conditions, respectively, and $K_\nu(x)$ is the MacDonal function. At large distances from the plate, $z_j \gg L_i$, the boundary-induced current density behaves as $\langle j^l \rangle_j^{(1)} \propto e^{-2\omega_0 z_j} / z_j^{(p+1)/2}$. The suppression is exponential for both massive and massless fields.

An important issue in quantum field theory with boundaries is the appearance of surface divergences in the VEVs of local physical observables. Examples of the latter are the VEVs of the field squared and of the energy density. These divergences are a consequence of the oversimplification of a model where the physical interactions are replaced by the imposition of boundary conditions for all modes of a fluctuating quantum field. Of course, this is an idealization, as real physical systems cannot constrain all the modes. The appearance of divergences in the VEVs of physical quantities indicates that a more realistic physical model should be employed for their evaluation on the boundaries. An important feature in the problem under consideration is that the VEV of the current density is finite on the plate. This is in sharp contrast with the behavior of the VEVs for the field squared and energy-momentum tensor. The finiteness of the current density on the boundary may be understood from general arguments. The divergences in local physical observables are determined by the local bulk and boundary geometries. If we consider the model with the topology $R^{p+2} \times T^{q-1}$ with the l th dimension having the topology R^1 , then in this model the l th component of the current density vanishes by the symmetry. The compactification of the l th dimension to S^1 does not change both the bulk end boundary local geometries and, hence, does not add new divergences to the VEVs compared with the model on $R^{p+2} \times T^{q-1}$. In the case of Dirichlet boundary condition the boundary-free and plate-induced parts of the current density cancel each other for $z_j = 0$ and, hence, the total current vanishes on the plate. For Neumann condition the current density on the plate is given by $\langle j^l \rangle_{j,z=a_j} = 2\langle j^l \rangle_0$. The normal derivative of the current density on the plate vanishes for both Dirichlet and Neumann boundary conditions: $(\partial_z \langle j^l \rangle_j)_{z=a_j} = 0$. This is not the case for general Robin condition.

The behavior of the plate-induced part of the current density along l th dimension, in the limit when the lengths of the other compact dimensions are much smaller than L_l , crucially depend whether the phases $\tilde{\alpha}_i$, $i \neq l$, are zero or not. For $\sum_{i \neq l} \tilde{\alpha}_i^2 \neq 0$ the plate-induced contribution is suppressed by the factor $e^{-L_l \omega_{0l}(1+2z_j^2/L_l^2)}$, where $\omega_{0l}^2 = \omega_0^2 - \tilde{\alpha}_l^2/L_l^2$. For $\tilde{\alpha}_i = 0$, $i \neq l$, the leading term in the asymptotic expansion, multiplied by V_q/L_l , coincides with the corresponding current density for $(p+2)$ -dimensional space with topology $R^{p+1} \times S^1$.

In figure 1, for the simplest Kaluza-Klein model with a single compact dimension of the length L ($D = 4$) and with the phase $\tilde{\alpha}$, we have plotted the total current density, $L^D \langle j^l \rangle_j / e$, for a massless scalar field in the geometry of a single plate as a function of the distance from the plate and of the phase $\tilde{\alpha}$. The left/right panel correspond to Dirichlet/Neumann boundary conditions. As has been already noticed before, in the Dirichlet case the total current density vanishes on the plate.

For the same model, figure 2 presents the plate-induced contribution to the current density as a function of the distance from the plate for various values of the coefficients in the Robin boundary condition (left panel) and as a function of the ratio β_j/L (right panel). The numbers near the curves on the right panel correspond to the value of β_j/L . The left panel is plotted for the fixed value of the relative distance from the plate $z_j/L = 0.3$. On both panels, the dashed curves are plotted for Dirichlet and Neumann boundary conditions. For the phase in the quasiperiodicity condition we have taken $\tilde{\alpha} = \pi/2$. On the right panel, for the values of β_j/L between the ordinate axis and the vertical dotted line ($\beta_j/L = 1/\tilde{\alpha}$) the vacuum is unstable.

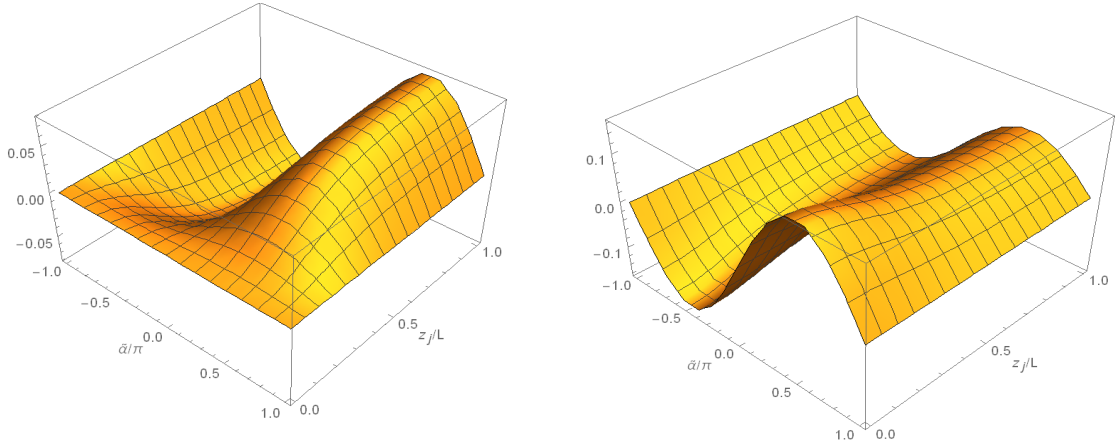


Figure 1: The total current density, $L^D \langle j^l \rangle_j / e$, in the topology $R^3 \times S^1$ for a $D = 4$ massless scalar field with Dirichlet (left panel) and Neumann (right panel) boundary conditions in the geometry of a single plate, as a function of the phase in the quasiperiodicity boundary condition and of the distance from the plate.

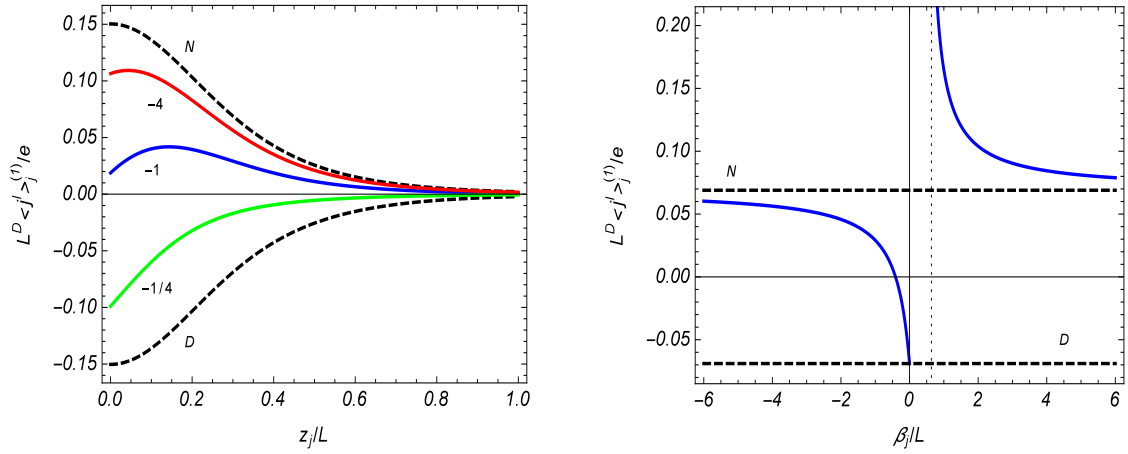


Figure 2: The plate-induced contribution to the current density for the model corresponding to figure 1 as a function of the distance from the plate (left panel) for different values of the ratio β_j/L (numbers near the curves) and as a function of β_j/L (right panel) for $z_j/L = 0.3$. The dashed curves correspond to Dirichlet and Neumann boundary conditions and the graphs are plotted for $\tilde{\alpha} = \pi/2$.

In Section 2.3 the VEV of the current density in the region between the plates ($a_1 \leq z \leq a_2$) is investigated. The expression for the component along the l th compact dimension reads

$$\langle j^l \rangle = \langle j^l \rangle_0 + \frac{e\pi^{-(p+1)/2}}{2^p \Gamma((p+1)/2) V_q} \sum_{\mathbf{n}_q} k_l \int_{\omega_{\mathbf{n}_q}}^{\infty} dy (y^2 - \omega_{\mathbf{n}_q}^2)^{\frac{p-1}{2}} \frac{2 + \sum_{j=1,2} c_j(ay) e^{2yz_j}}{c_1(ay)c_2(ay)e^{2ay} - 1}, \quad (17)$$

where $a = a_2 - a_1$ and $c_j(u) = (b_j u - 1)/(b_j u + 1)$, $b_j = \beta_j/a$. In the case of Dirichlet boundary condition the total current vanishes on the plates: $\langle j^l \rangle_{z=a_j} = 0$. The normal derivative vanishes on the plates for both Dirichlet and Neumann cases. In the limit when the separation between the plates is smaller than all the length scales in the problem, the behavior of the current density is essentially different for non-Neumann and Neumann boundary conditions. In the former case, the total current density in the region between the plates tends to zero. For Neumann boundary condition on both plates, for small separations the total current density is dominated by the interference part and it diverges inversely proportional to the separation.

In figure 3, in the model with a single compact dimension of the length L and for a $D = 4$ massless scalar field with Dirichlet (left panel) and Neumann (right panel) boundary conditions, the total current density in the region between the plates located at $z = 0$ and $z = a$ is plotted as a function of the ratio z/a . The numbers near the curves correspond to the values of a/L and the graphs are plotted for $\tilde{\alpha} = \pi/2$. The current density for Dirichlet/Neumann scalar decreases/increases with decreasing separation between the plates and for Dirichlet scalar it vanishes on the plates.

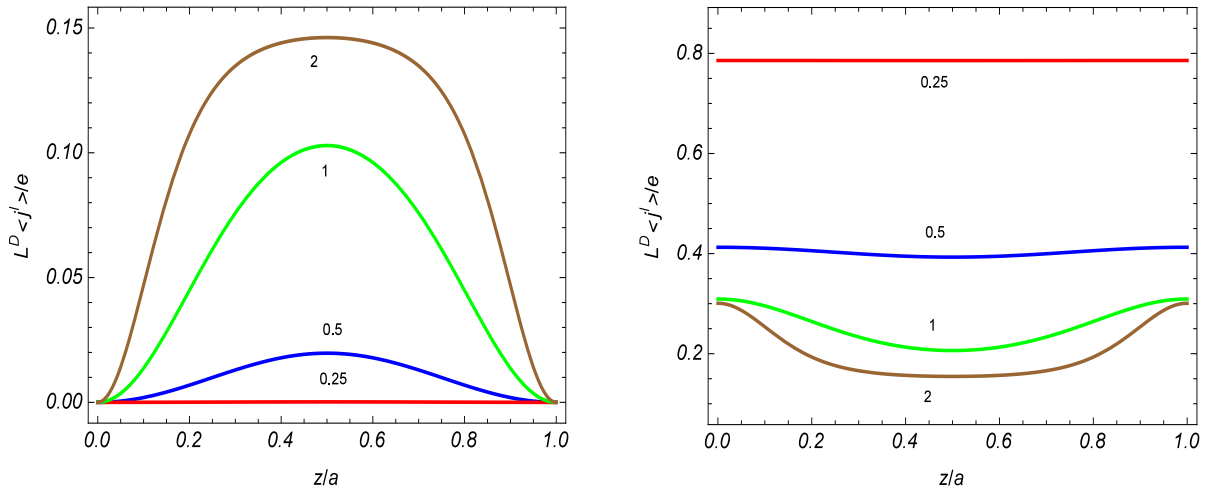


Figure 3: The current density between the plates as a function of the relative distance from the left plate in the model with a single compact dimension. The graphs are plotted for a massless field with the parameter $\tilde{\alpha} = \pi/2$ and with Dirichlet (left panel) and Neumann (right panel) boundary conditions. The numbers near the curves correspond to the values of a/L .

The same graphs for Dirichlet boundary condition on the left plate and Neumann condition on the right one are presented on the left panel of figure 4. The right panel in figure 4 is plotted for Robin boundary condition on both plates with $\beta_1/L = \beta_2/L = -1$. In the Robin case, the current density decreases with the further decrease of the separation between the plates and it tends to zero in the limit $a \rightarrow 0$, in accordance with the general analysis described above.

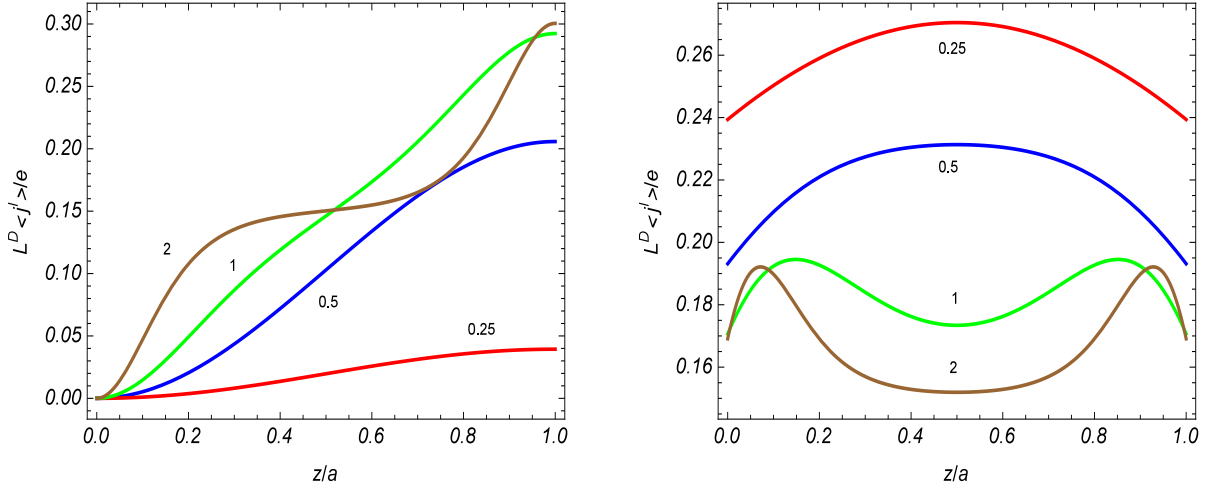


Figure 4: The same as in figure 4 for Dirichlet boundary condition on the left plate and Neumann condition on the right one (left panel). The right panel is plotted for Robin boundary condition on both plates with $\beta_1/L = \beta_2/L = -1$.

The results may be applied to Kaluza-Klein-type models in the presence of branes (for $D > 3$) and to planar condensed matter systems (for $D = 2$), described within the framework of an effective field theory. In particular, in the former case, the vacuum currents along compact dimensions generate magnetic fields in the uncompactified subspace. The boundaries discussed above can serve as a simple model for the edges of planar systems.

Chapter 3 is devoted to the study of the effects of gravitational field and of a cylindrical shell on local characteristics of the electromagnetic vacuum. As a background geometry we take $(D + 1)$ -dimensional dS spacetime with the line element

$$ds^2 = dt^2 - e^{2t/\alpha} [dr^2 + r^2 d\phi^2 + (d\mathbf{z})^2], \quad (18)$$

where $\mathbf{z} = (z^3, \dots, z^D)$. The parameter α is expressed in terms of the cosmological constant Λ as $\alpha^2 = D(D - 1)/(2\Lambda)$. On the cylindrical surface $r = a$ the field obeys the boundary condition $n^{\nu_1} *F_{\nu_1 \dots \nu_{D-1}} = 0$, where n^ν is the normal to the boundary, $*F_{\nu_1 \dots \nu_{D-1}}$ is the dual of the electromagnetic field tensor $F_{\mu\nu} = \partial_\mu A_\nu - \partial_\nu A_\mu$. For $D = 3$ that condition reduces to the boundary condition on the surface of a perfect conductor. The complete set of the electromagnetic field cylindrical modes are specified inside and outside of the cylindrical shell. In the special case $D = 3$ and in the Minkowskian limit they are reduced to the well known TE and TM modes in cylindrical waveguides. In the $(D + 1)$ -dimensional case one has a single mode of the TE type and $D - 2$ modes of the TM type.

As a local characteristic of the vacuum state we consider the VEV of the squared electric field. This VEV is obtained by making use of the mode-sum over the complete set of the electromagnetic field mode functions and is decomposed as $\langle E^2 \rangle = \langle E^2 \rangle_{\text{dS}} + \langle E^2 \rangle_{\text{b}}$, where $\langle E^2 \rangle_{\text{dS}}$ corresponds to the VEV in dS spacetime in the absence of boundaries. The part of the VEV $\langle E^2 \rangle_{\text{b}}$ is induced by the presence of the cylindrical boundary and in the region $r < a$ is

given by the expression

$$\begin{aligned} \langle E^2 \rangle_b &= \frac{2^5 (4\pi)^{-D/2}}{\Gamma(D/2 - 1) \alpha^{D+1}} \sum_{m=0}^{\infty} \sum_{\lambda=0,1} \int_0^{\infty} dx x^{D+1} \frac{K_m^{(\lambda)}(xa/\eta)}{I_m^{(\lambda)}(xa/\eta)} \\ &\times \int_0^1 ds s (1-s^2)^{D/2-2} G_m^{(\lambda)}[s, I_m(xr/\eta)] f_{D/2-2}(xs), \end{aligned} \quad (19)$$

with the notations $\eta = \alpha e^{-t/\alpha}$, $f_\nu(x) = K_\nu(x) [I_{-\nu}(x) + I_\nu(x)]$ and

$$G_m^{(\lambda)}[s, f(x)] = \begin{cases} (1-s^2) [f'^2(x) + m^2 f^2(x)/x^2] + [s^2(D-3) + 1] f^2(x), & \lambda = 0, \\ -s^2 [f'^2(x) + m^2 f^2(x)/x^2], & \lambda = 1. \end{cases} \quad (20)$$

In (19), $I_m(z)$ is the modified Bessel function, $I_m^{(0)}(z) = I_m(z)$, $I_m^{(1)}(z) = I'_m(z)$ and the same for $K_m^{(\lambda)}(z)$. Note that $\tau = -\eta$ is the conformal time coordinate. The expression for $\langle E^2 \rangle_b$ in the region $r > a$ is obtained from (19) by the interchange $I_m \rightleftharpoons K_m$. In both the interior and exterior regions the shell-induced contributions depend on the variables η , a , r in the form of the ratios a/η and r/η . This feature is a consequence of the maximal symmetry of dS spacetime. Note that the combination $\alpha a/\eta$ is the proper radius of the cylindrical shell and, hence, a/η is the proper radius measured in units of the dS curvature scale α . Similarly, the ratio r/η is the proper distance from the cylinder axis measured in units of α . The presence of the boundary does not change the local geometry for points outside the shell. This means that at those points the divergences are the same in both the problems, in the absence and in the presence of the cylindrical shell. From here it follows that the divergences are contained in the part $\langle E^2 \rangle_{\text{dS}}$ only, whereas the boundary-induced contribution $\langle E^2 \rangle_b$ is finite for points away from the boundary. Hence, the renormalization is required for the boundary-free part only. It can be shown that $\langle E^2 \rangle_b$ is always positive.

The VEV of the electric field squared for a cylindrical shell in Minkowski spacetime, $\langle E^2 \rangle_b^{(M)}$, is obtained by the limiting transition $\alpha \rightarrow \infty$ for a fixed value of t . In the special case of 4-dimensional dS spacetime one has $D = 3$ and we get $\langle E^2 \rangle_b = (\eta/\alpha)^4 \langle E^2 \rangle_b^{(M)}$. In this case, the VEV of the field squared is related to the corresponding result in Minkowski spacetime by standard conformal transformation with the conformal factor $(\eta/\alpha)^4$. This is a direct consequence of the conformal invariance of the electromagnetic field in $D = 3$ spatial dimensions and of the conformal flatness of the background geometry. Near the shell, to the leading order one finds

$$\langle E^2 \rangle_b \approx \frac{3(D-1)\Gamma((D+1)/2)}{2^D \pi^{(D-1)/2} |\alpha(a-r)/\eta|^{D+1}}, \quad (21)$$

where $|\alpha(a-r)/\eta|$ is the proper distance from the boundary. The leading term (21) is obtained from that for the cylindrical shell with the radius a in Minkowski spacetime by the replacement $(a-r) \rightarrow \alpha(a-r)/\eta$. For points near the boundary the contribution of the modes with small wavelengths dominate and at distances from the shell smaller than the curvature radius of the dS spacetime the influence of the gravitational field is small.

At large proper distances from the shell compared with the dS curvature radius, we have $r/\eta \gg 1$. For even $D > 4$ one gets

$$\langle E^2 \rangle_b \approx \frac{4(4D^2 - 3D - 4)\Gamma^3(D/2 + 1)}{\pi^{D/2} D(D-4)\Gamma(D+2)} \frac{\alpha}{(\alpha r/\eta)^{D+2} \ln(r/a)}. \quad (22)$$

In the cases $D = 3, 4, 5$ the leading terms are given by

$$\langle E^2 \rangle_{\text{b}}|_{D=3} \approx \frac{2(\alpha r/\eta)^{-4}}{3\pi \ln(r/a)}, \quad \langle E^2 \rangle_{\text{b}}|_{D=4} \approx \frac{16\pi^{-2}\alpha(\alpha r/\eta)^{-6}}{5 \ln(r/a) \ln(r/\eta)}, \quad \langle E^2 \rangle_{\text{b}}|_{D=5} \approx \frac{7(\alpha r/\eta)^{-6}}{10\pi^2 \ln(r/a)}.$$

At large distances, the total VEV is dominated by the boundary-free part $\langle E^2 \rangle_{\text{dS}}$. For a cylindrical shell in the Minkowski bulk, at large distances, $r \gg a$, one has $\langle E^2 \rangle_{\text{b}}^{(\text{M})} \propto 1/[r^{D+1} \ln(r/a)]$ for all $D \geq 3$. In figure 5, for the model with $D = 4$ the shell-induced contribution is plotted versus the proper distance from the shell axis, measured in units of α . For the proper radius of the shell, in the same units, we have taken $a/\eta = 2$. The corresponding Casimir-Polder force is expressed in terms of the derivative $\partial_r \langle E^2 \rangle_{\text{b}}$. This force is directed toward the cylindrical shell.

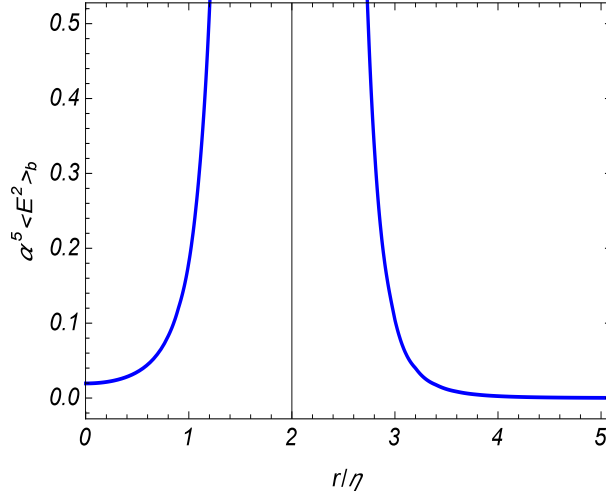


Figure 5: Shell-induced contribution in the VEV of the squared electric field versus the proper distance from the shell axis for the $D = 4$ model. For the corresponding value of the shell radius we have taken $a/\eta = 2$.

Another important local characteristic of the vacuum state is the VEV of the energy-momentum tensor. The VEV of the energy-momentum tensor is presented in the form $\langle T_\mu^\nu \rangle = \langle T_\mu^\nu \rangle_{\text{dS}} + \langle T_\mu^\nu \rangle_{\text{b}}$, where $\langle T_\mu^\nu \rangle_{\text{dS}}$ is the corresponding VEV in the boundary-free dS spacetime and the contribution $\langle T_\mu^\nu \rangle_{\text{b}}$ is induced by the presence of the cylindrical shell. For points outside the cylindrical shell the boundary-induced contribution is finite and the renormalization is reduced to the one for the boundary-free part. From the maximal symmetry of dS spacetime it follows that the latter does not depend on the spacetime point and has the form $\langle T_\mu^\nu \rangle_{\text{dS}} = \text{const} \cdot \delta_\mu^\nu$. In the region $r < a$ for the boundary-induced parts in the diagonal components we get (no summation over i)

$$\begin{aligned} \langle T_i^i \rangle_{\text{b}} &= \frac{B_D}{\alpha^{D+1}} \sum_{m=0}^{\infty} \sum_{\lambda=0,1} \int_0^\infty dx x^{D+1} \frac{K_m^{(\lambda)}(ax/\eta)}{I_m^{(\lambda)}(ax/\eta)} \int_0^1 ds s \\ &\times (1-s^2)^{D/2-2} \sum_{l=0,1} P_{\lambda l}^{(i)}[s, I_m(xr/\eta)] f_{D/2-1-l}(xs), \end{aligned} \quad (23)$$

where $B_D = 2^{2-D} \pi^{-D/2-1} / \Gamma(D/2 - 1)$ and we have defined the functions

$$P_{\lambda l}^{(i)}[s, f(y)] = (A_{\lambda l}^{(i)} + B_{\lambda l}^{(i)} s^2) Z_m^{(i)}[f(y)] + (C_{\lambda l}^{(i)} + (D-3) D_{\lambda l}^{(i)} s^2) f^2(y), \quad (24)$$

$$\begin{aligned}
Z_m^{(i)}[f(y)] &= f'^2(y) + m^2 f^2(y)/y^2, \quad i = 0, 3, \dots, D, \\
Z_m^{(i)}[f(y)] &= f'^2(y) - m^2 f^2(y)/y^2, \quad i = 1, 2.
\end{aligned} \tag{25}$$

The numerical coefficients $F_{\lambda_l}^{(i)}$ in (24), with $F = A, B, C, D$ depend on the number of spatial dimensions D only. In addition to the diagonal component, the VEV of the energy-momentum tensor has a nonzero off-diagonal component $\langle T_0^1 \rangle$. This component describes energy flux along the radial direction (along the direction normal to the boundary). It is induced by the presence of the shell and in the region $r < a$ is given by the expression

$$\begin{aligned}
\langle T_0^1 \rangle_b &= -\frac{2B_D}{\alpha^{D+1}} \sum_{m=0}^{\infty} \int_0^{\infty} dx x^{D+1} \left[(D-2) \frac{K_m(xa/\eta)}{I_m(xa/\eta)} - \frac{K'_m(xa/\eta)}{I'_m(xa/\eta)} \right] I_m(xr/\eta) I'_m(xr/\eta) \\
&\times \int_0^1 ds s^2 (1-s^2)^{D/2-2} [K_{D/2-1}(y) I_{2-D/2}(y) - K_{D/2-2}(y) I_{D/2-1}(y)]_{y=xs}. \tag{26}
\end{aligned}$$

In the special case $D = 3$ the off-diagonal component vanishes. For other values of D , for which the representation (26) is valid, $\langle T_0^1 \rangle_b < 0$ for $0 < r < a$. On the axis, the energy flux vanishes, $\langle T_0^1 \rangle_{b,r=0} = 0$. Similar to the case of the field squared, the boundary-induced VEVs (23) and (26) depend on η, a, r in the form of the ratios a/η and r/η . The expressions for the components of the vacuum energy-momentum tensor in the region $r > a$ are obtained from (23) and (26) by the replacements $I_m \rightleftharpoons K_m$.

In the special case $D = 3$ the off-diagonal component of the vacuum energy-momentum tensor vanishes, $\langle T_0^1 \rangle_b = 0$, and the diagonal components are connected to the corresponding quantities for a cylindrical shell in the Minkowski bulk by the relation (no summation over i) $\langle T_i^i \rangle_b = (\eta/\alpha)^4 \langle T_i^i \rangle_b^{(M)}$. Near the cylindrical shell, the leading terms are given by the expressions (no summation over i)

$$\langle T_i^i \rangle_b \approx -\frac{(D-1)(D-3)\Gamma((D+1)/2)}{2(4\pi)^{(D+1)/2} |\alpha(a-r)/\eta|^{D+1}}, \tag{27}$$

for $i = 0, 2, \dots, D$, and $\langle T_0^1 \rangle_b \approx \langle T_0^0 \rangle_b (a-r)/\eta$, $\langle T_1^1 \rangle_b \approx \langle T_0^0 \rangle_b (a-r)/(Da)$. The leading terms for the diagonal components coincide with those for a cylindrical shell in Minkowski bulk with the distance from the shell replaced by the proper distance $|\alpha(a-r)/\eta|$. In the special case $D = 3$ the leading terms vanish. The latter feature is related to the conformal invariance of the electromagnetic field in $D = 3$.

In figure 6 we have plotted the boundary-induced contribution in the energy density and the energy flux as functions of the proper distance from the shell axis, measured in units of the dS curvature scale α . For the corresponding value of the shell radius we have taken $a/\eta = 2$. As is seen, in the interior region the energy density is negative near the shell and positive near the axis of the shell. The energy flux is negative inside the shell. This means that the energy flux is directed from the shell. The corresponding energy density in the Minkowski bulk is negative everywhere.

Another boundary condition, used for the confinement of gauge fields in bag models of hadrons and in flux tube models of QCD, is the one given by $n^\mu F_{\mu\nu} = 0$. The corresponding expressions for the VEVs of the field squared and energy-momentum tensor are obtained from those for generalized perfect conductor boundary condition by the replacement

$$\frac{K_m^{(\lambda)}(xa/\eta)}{I_m^{(\lambda)}(xa/\eta)} \rightarrow \frac{K_m^{(1-\lambda)}(xa/\eta)}{I_m^{(1-\lambda)}(xa/\eta)}. \tag{28}$$

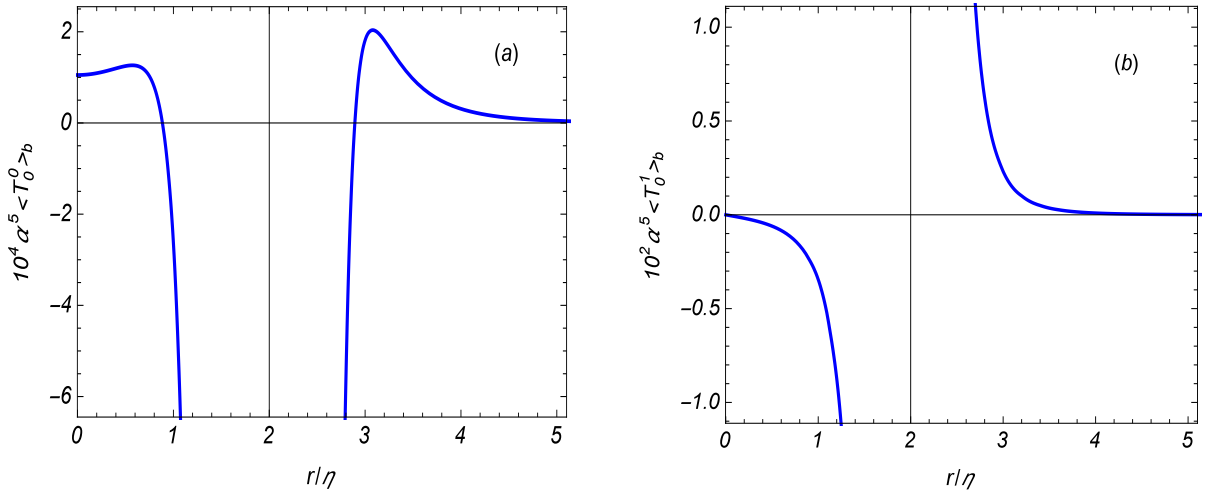


Figure 6: Shell-induced contribution in the VEV of the energy density (panel (a)) and the energy flux (panel (b)) as functions of the ratio r/η in the $D = 4$ model. The graphs are plotted for $a/\eta = 2$.

In this case, the boundary-induced contribution on the VEV of the squared electric field is neagtive in both the interior and exterior regions.

In Chapter 4 the electromagnetic field vacuum fluctuations are investigated around a straight cosmic string in background of dS spacetime. Although the specific properties of cosmic strings are model-dependent, they produce similar gravitational effects. In the simplified model with the string induced planar angle deficit, the nontrivial spatial topology results in the distortion of the vacuum fluctuations spectrum of quantized fields and induces shifts in VEVs of physical characteristics of the vacuum state. The line element of the background geometry is given by (18) where now $0 \leq \phi \leq \phi_0$. In the case $\phi_0 < 2\pi$, though the local geometrical characteristics for $r \neq 0$ remain the same, the global properties are different. The special case $D = 3$ corresponds to a straight cosmic string with the core along the axis z^3 and with the planar angle deficit $2\pi - \phi_0$ determined by the linear mass density of the string.

By using the summation over the complete set of the electromagnetic field modes, the two-point functions for the electric and magnetic fields products are evaluated. The contributions corresponding to dS spacetime in the absence of the cosmic string are explicitly extracted. In the model of the cosmic string under consideration the local geometrical characteristics outside the string core are not changed by the presence of the string. Consequently, the divergences and the renormalization procedure for the VEVs are the same as those in pure dS spacetime. The topological parts do not require a renormalization. The renormalized VEVs for the squared electric ($F = E$) and magnetic ($F = M$) fields are presented in the decomposed form

$$\langle F^2 \rangle = \langle F^2 \rangle_{\text{dS}} + \frac{8\alpha^{-D-1}}{(2\pi)^{D/2}} \left[\sum_{l=1}^{[q/2]} g_F(r/\eta, s_l) - \frac{q}{\pi} \sin(q\pi) \int_0^\infty dy \frac{g_F(r/\eta, \cosh y)}{\cosh(2qy) - \cos(q\pi)} \right], \quad (29)$$

where $q = 2\pi/\phi_0$, $s_l = \sin(\pi l/q)$, $[q/2]$ is the integer part of $q/2$. In (29), $\langle F^2 \rangle_{\text{dS}}$ is the renormalized VEV in the absence of the cosmic string and the remaining part is induced by

the cosmic string (topological part) and

$$\begin{aligned}
g_E(x, y) &= \int_0^\infty du u^{D/2} K_{D/2-2}(u) e^{u-2x^2y^2u} [2ux^2y^2 (2y^2 - D + 1) + (D - 1) (D/2 - 2y^2)], \\
g_M(x, y) &= \int_0^\infty du u^{D/2} K_{D/2-1}(u) e^{u-2x^2y^2u} \{ (D - 1)D/2 \\
&\quad - 4(D - 2)y^2 + 2x^2y^2u [2(D - 2)y^2 - D + 1] \}.
\end{aligned} \tag{30}$$

If the parameter q is equal to an even integer the term $l = q/2$ in (29) should be taken with an additional coefficient $1/2$. The VEV (29) depends on r and η in the form of the combination r/η . The latter property is a consequence of the maximal symmetry of dS spacetime. Note that, for a given η , the ratio $\alpha r/\eta$ is the proper distance from the string. Hence, r/η is the proper distance measured in units of the dS curvature scale α . From the maximal symmetry of dS spacetime we expect that the pure dS part does not depend on the spacetime point and $\langle F^2 \rangle_{\text{dS}} = \text{const} \cdot \alpha^{-D-1}$.

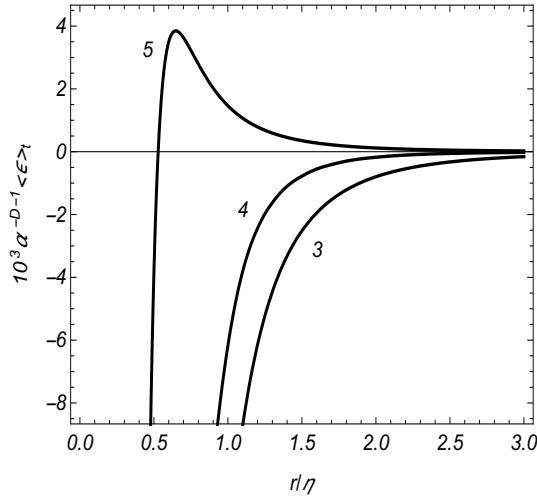


Figure 7: Topological contributions in the VEV of the energy density in spatial dimensions $D = 3, 4, 5$ (the numbers near the curves) for $q = 2.5$.

For odd D , the functions $g_F(x, y)$, $F = E, M$, are expressed in terms of the elementary functions. In particular, for $D = 3$ one has

$$\langle F^2 \rangle = \langle F^2 \rangle_{\text{dS}} - \frac{(q^2 - 1)(q^2 + 11)}{180\pi(\alpha r/\eta)^4}, \tag{31}$$

and for $D = 5$

$$\begin{aligned}
\langle E^2 \rangle &= \langle E^2 \rangle_{\text{dS}} - \frac{(q^2 - 1)(q^4 + 22q^2 + 211)}{1890\pi^2(\alpha r/\eta)^6}, \\
\langle B^2 \rangle &= \langle B^2 \rangle_{\text{dS}} + \frac{q^2 - 1}{1890} \frac{21(q^2 + 11)r^2/\eta^2 - 2q^4 + 40q^2 + 502}{2\pi^2(\alpha r/\eta)^6}.
\end{aligned} \tag{32}$$

At large distances from the string, $r/\eta \gg 1$, the topological part in the VEV of the electric field squared decays as $(\eta/r)^4$ for $D = 3$, as $\ln(r/\eta)(\eta/r)^6$ for $D = 4$ and as $(\eta/r)^6$ for $D > 4$. The VEV of the magnetic field squared decays as $(r/\eta)^4$ for $D \neq 4$ and as $(r/\eta)^6$ for $D = 4$. The pure

dS part $\langle F^2 \rangle_{\text{dS}}$ is a constant and it dominates in the total VEV at large distances. Note that at large distances from the string the influence of the gravitational field on the VEV is essential. In the Minkowskian case the decay of the VEV is as $1/r^{D+1}$ and depends on the number of spatial dimension.

Having the VEVs for the squared electric and magnetic fields, we can find the VEV of the energy density ε as $\langle \varepsilon \rangle = (\langle E^2 \rangle + \langle B^2 \rangle)/(8\pi)$. Depending on the parameters D and q , the topological part in the energy density can be either negative or positive. For $D = 3$ it is always negative. At large distances from the cosmic string and for $D > 4$ the topological contribution in the energy density is dominated by the magnetic part and decays as $(\eta/r)^4$. For $D = 4$ and at large distances the electric part dominates and the energy density decays like $(\eta/r)^6 \ln(r/\eta)$. In figure 7 we display the dependence of the topological contribution in the vacuum energy density as a function of the proper distance from the string (measured in units of dS curvature scale). The graphs are plotted for spatial dimensions $D = 3, 4, 5$. As is seen, in general, the energy density is not a monotonic function of the distance from the string. Moreover, in the case $D = 5$ the energy density changes the sign: it is negative near the string (the electric part dominates) and positive at large distances from the string (the magnetic contribution dominates).

CONCLUSIONS

1. For a scalar field with Robin boundary condition on a spherical shell in the background of a constant negative curvature space the Wightman function, the mean field squared and the VEV of the energy-momentum tensor are decomposed into the boundary-free and sphere-induced contributions. This reduces the renormalization procedure to the one for the space without boundaries. The corresponding results are generalized for spaces with spherical bubbles and for cosmological models with negative curvature spaces. For the coefficient in the boundary condition there is a critical value above which the scalar vacuum becomes unstable.
2. At distances from the sphere larger than the curvature scale of the background space the suppression of the vacuum fluctuations in the gravitational field corresponding to the negative curvature space is stronger compared with the case of the Minkowskian bulk. The decay of the VEVs with the distance is exponential for both massive and massless fields.
3. For a charged scalar field in spacetimes with toroidally compactified spatial dimensions and in the presence of planar boundaries, the nontrivial phases in quasiperiodicity conditions along compact dimensions and a constant gauge field induce vacuum current density. It is a periodic function of the magnetic flux, enclosed by compact dimensions, with the period equal to the flux quantum.
4. The current density does not contain surface divergences and for Dirichlet condition it vanishes on the boundaries. The normal derivative of the current density on the boundaries vanishes for both Dirichlet and Neumann conditions. There is a region in the space of the parameters in Robin boundary conditions where the vacuum state becomes unstable. The stability condition depends on the lengths of compact dimensions and is less restrictive than that for background with trivial topology.

5. Complete set of cylindrical modes is constructed for the electromagnetic field inside and outside a cylindrical shell in the background of $(D + 1)$ -dimensional dS spacetime and the VEVs of the electric field squared and of the energy-momentum tensor are evaluated for the Bunch-Davies vacuum state. The shell-induced contribution in the electric field squared is positive for both the interior and exterior regions and the corresponding Casimir-Polder forces are directed toward the shell. The vacuum energy-momentum tensor, in addition to the diagonal components, has a nonzero off-diagonal component corresponding to the energy flux along the direction normal to the shell. The flux is directed from the shell in both the exterior and interior regions. The results are extended for confining boundary conditions of flux tube models in quantum chromodynamics.
6. The electromagnetic field correlators around a cosmic string in dS spacetime are presented in the form where the string-induced topological parts are explicitly extracted. With this decomposition, the renormalization of the local VEVs in the coincidence limit is reduced to the one for dS spacetime in the absence of the cosmic string. Near the string the VEVs of the squared electric and magnetic fields, and of the vacuum energy density are dominated by the topological contributions and the effects induced by the gravitational field are small. At distances from the string larger than the curvature radius of the background geometry, the pure dS parts in the VEVs dominate. In this region the influence of the gravitational field on the topological contributions is crucial and the corresponding behavior is essentially different from that for a cosmic string on the Minkowski bulk.
7. It is argued that, as a consequence of the quantum-to-classical transition of super-Hubble electromagnetic fluctuations during cosmological inflation, in the postinflationary era these strings will be surrounded by large scale stochastic magnetic fields. These fields could be among the distinctive features of the cosmic strings produced during the inflation and also of the corresponding inflationary models.

REFERENCES

1. M. Bordag, G.L. Klimchitskaya, U. Mohideen, V.M. Mostepanenko, *Advances in the Casimir Effect* (Oxford University Press, Oxford, 2009).
2. *Casimir Physics*, edited by D. Dalvit, P. Milonni, D. Roberts, F. da Rosa, *Lecture Notes in Physics* Vol. 834 (Springer-Verlag, Berlin, 2011).
3. A. Cortijo, F. Guinea, M.A.H. Vozmediano, Geometrical and topological aspects of graphene and related materials. *J. Phys. A: Math. Theor.* **45**, 383001 (2012).
4. A. Iorio and G. Lambiase, Quantum field theory in curved graphene spacetimes, Lobachevsky geometry, Weyl symmetry, Hawking effect, and all that. *Phys. Rev. D* **90**, 025006 (2014).
5. R. Jackiw, S.-Y. Pi, Chiral gauge theory for graphene. *Phys. Rev. Lett.* **98**, 266402 (2007).
6. O. Oliveira, C.E. Cordeiro, A. Defino, W. de Paula, T. Frederico, Vortex and gap generation in gauge models of graphene. *Phys. Rev. B* **83**, 155419 (2011).
7. E.R. Bezerra de Mello, A.A. Saharian, Finite temperature current densities and Bose-Einstein condensation in topologically nontrivial spaces. *Phys. Rev. D* **87**, 045015 (2013).

PUBLICATIONS IN THE TOPIC OF THESIS

1. S. Bellucci, A. A. Saharian, N. A. Saharyan, Wightman function and the Casimir effect for a Robin sphere in a constant curvature space, *Eur. Phys. J. C* **74**, 3047 (2014), 19 pages.
2. S. Bellucci, A. A. Saharian, N. A. Saharyan, Casimir effect for scalar current densities in topologically nontrivial spaces, *Eur. Phys. J. C* **75**, 378 (2015), 17 pages.
3. A. A. Saharian, V. F. Manukyan, N. A. Saharyan, Electromagnetic Casimir densities for a cylindrical shell on de Sitter space, *Int. J. Mod. Phys. A* **31**, No. 34, 1650183 (2016), 29 pages.
4. A. A. Saharian, V. F. Manukyan, N. A. Saharyan, Electromagnetic vacuum fluctuations around a cosmic string in de Sitter spacetime, *Eur. Phys. J. C* **77**, 478 (2017), 13 pages.
5. N. A. Saharyan, Casimir densities outside a constant curvature spherical bubble. *Armenian Journal of Physics* **10** (3), 112-121 (2017).
6. A. A. Saharian, V. F. Manukyan, N. A. Saharyan, Electromagnetic vacuum densities induced by cosmic string. *Particles* **1**, 13 (2018), 19 pages.
7. A. S. Kotanjyan, R. M. Avagyan, G. H. Harutunyan, N. A. Saharyan, Dynamics of the quasi-de Sitter model of the Early Universe. *Physics of Atomic Nuclei* **81**, 894-898 (2018).

ԱՄՓՈՓԱԳԻՐ

Հետազոտված է դասական գրավիտացիոն դաշտի, սահմանների և ոչ-տրիվիալ տոպոլոգիայի ազդեցությունը քվանտային վակուումի հատկությունների վրա սկալյար և էլեկտրամագնիսական դաշտերի համար: Հաշվարկված են սկալյար դաշտի Վայթմանի ֆունկցիան, դաշտի քառակուսու և էներգիա-իմպուլսի թենզորի վակուումային միջինները հաստատուն բացասական կորությամբ տարածությունում սֆերայի ներսում և դրսում: Սահմանով մակաձված ներդրումների համար ստացված են արագ զուգամիտող ինտեգրալ ներկայացումներ: Գրավիտացիոն դաշտի ազդեցությունը վակուումային միջինների վրա էական է սֆերայից տարածության կորության շառավղից մեծ հեռավորությունների վրա: Լիցքավորված սկալյար դաշտի համար ուսումնասիրված են Հադամարի ֆունկցիան և հոսանքի խտության վակուումային միջինը տորոիդալ կոմպակտիֆիկացված տարածական չափողականություններով հարթ տարածաժամանակում, հաստատուն տրամաչափային դաշտի և հարթ զուգահեռ սահմանների առկայությամբ: Կոմպակտ չափերի երկայնքով դաշտի օպերատորը բավարարում է կամայական փուլերով քվադրապրերականության պայմանների, իսկ սահմանների վրա դրվում են Ռոբինի եզրային պայմաններ: Վակուումային հոսանքի խտությունը ոչ-գրոյական բաղադրիչներ ունի միայն կոմպակտ չափերի ուղղությամբ: Ստացված են էլեկտրամագնիսական դաշտի գլանային մոդուլները դե Միտտերի տարածությունում գլանային թաղանթի առկայությամբ: Դրանց հիման վրա հետազոտված են էլեկտրական դաշտի քառակուսու և էներգիա-իմպուլսի թենզորի վակուումային միջինները: Միջիններում բացահայտ առանձնացված են թաղանթով մակաձված ներդրումները և քննարկվում է դրանց վարքը տարբեր սահմանային դեպքերում: Հետազոտված են էլեկտրամագնիսական դաշտի երկկետային ֆունկցիաները, էլեկտրական ու մագնիսական դաշտերի քառակուսիների և էներգիայի խտության վակուումային միջինները դե Միտտերի տարածությունում կոսմիկական լարի շրջակայքում: Ցույց է տրված, որ լարին մոտ կետերում գրավիտացիոն դաշտի ազդեցությունը վակուումային միջինների վրա թույլ է, մինչդեռ տարածության կորության շառավղից մեծ հեռավորությունների վրա այդ ազդեցությունը էական է:

1. Հաստատուն բացասական կորությամբ ֆոնային տարածությունում գտնվող սֆերայի վրա Ռոբինի եզրային պայմանին բավարարող սկալյար դաշտի Վայթմանի ֆունկցիայում, դաշտի քառակուսու և էներգիա-իմպուլսի թենզորի վակուումային միջիններում բացահայտ առանձնացված են սահմանով մակաձված ներդրումները: Արդյունքում, վակուումային միջինների վերանորմավորումը հանգում է դրանց վերանորմավորմանը առանց սահմանի երկրաչափությունում: Համապատասխան արդյունքները ընդհանրացված են սֆերիկ պոլյաչակով տարածությունների և բացասական կորությամբ կոսմոլոգիական մոդելների համար: Առկա է եզրային պայմանի գործակցի կրիտիկական արժեք, որից մեծ արժեքների տիրույթում սկալյար վակուումը դառնում է անկայուն:
2. Սֆերայից՝ ֆոնային տարածության կորության շառավղից մեծ հեռավորությունների վրա վակուումային միջիններում սահմանով մակաձված ներդրումները բացասական կորությամբ տարածությունում ձգտում են գրոյի ավել արագ, քան Մինկովսկու երկրաչափությունում: Դրանք նվազում են էքսպոնենցիալ օրենքով ինչպես զանգվածեղ, այնպես էլ գրոյական զանգվածով դաշտերի համար:
3. Տորոիդալ կոմպակտիֆիկացված տարածական չափերով և հարթ սահմաններով ֆոնի վրա լիցքավորված սկալյար դաշտի համար կոմպակտ չափերի երկայնքով

քվագիպարբերականության պայմաններում ոչ տրիվիալ փուլերը և հաստատուն տրամաչափային դաշտը մակաձում են վակուումային հոսանքի խտություն: Այն պարբերական ֆունկցիա է կոմպակտ չափերով պարփակված մագնիսական հոսքից՝ հոսքի քվանտին հավասար պարբերությամբ:

4. Հոսանքի խտությունը չի պարունակում մակերևութային տարամիտություններ և զրո է սահմանների վրա Դիրիխլեի պայմանի դեպքում: Սահմանների վրա հոսանքի խտության նորմալ ածանցյալը զրո է է Դիրիխլեյի և Նեյմանի պայմանների համար: Ռոբինի եզրային պայմանների պարամետրերի տարածությունում առկա է տիրույթ, որտեղ վակուումային վիճակը դառնում է անկայուն: Կայունության պայմանը կախված է կոմպակտ չափերի երկարությունից և ավելի թույլ է քան տրիվիալ տոպոլոգիայով տարածությունում:
5. Ստացված են էլեկտրամագնիսական դաշտի գլանային մոդաների լրիվ դասերը դե Սիտտերի ֆոնային տարածաժամանակում գտնվող գլանային թաղանթի ներսում ու դրսում, հաշվարկվել են էլեկտրական դաշտի քառակուսու և էներգիա-իմպուլսի թենզորի վակուումային միջինները: Թաղանթով մակաձված մասի ներդրումը էլեկտրական դաշտի քառակուսու միջինում դրական է ինչպես ներքին, այնպես էլ արտաքին տիրույթներում և համապատասխան Կազիմիր-Պոլդերի ուժերը ուղղված են դեպի թաղանթը: Վակուումային էներգիա-իմպուլսի թենզորը բացի անկյունագծային բաղադրիչներից ունի նաև զրոյից տարբեր ոչ-անկյունագծային բաղադրիչ, որը համապատասխանում է թաղանթի նորմալի ուղղությամբ էներգիայի հոսքի: Հոսքը ուղղված է թաղանթից թե արտաքին և թե ներքին տիրույթներում: Արդյունքներն ընդհանրացված են քվանտային քրոմոդինամիկայում օգտագործվող թակարդող եզրային պայմանների համար:
6. Դե Սիտտերի տարածաժամանակում կոսմոլոգիական լարի շրջակայքում էլեկտրամագնիսական դաշտի կորեյատորների համար ստացված են արտահայտություններ, որոնցում բացահայտ առանձնացված են լարով մակաձված տոպոլոգիական ներդրումները: Դրա շնորհիվ համընկման սահմանում լոկալ վակուումային միջինների վերանորմավորումը հանգում է առանց կոսմոլոգիական լարի դե Սիտտերի տարածությունում վերանորմավորմանը: Լարին մոտ տիրույթում էլեկտրական ու մագնիսական դաշտերի քառակուսիների և էներգիայի խտության վակուումային միջիններում գերակշռում են տոպոլոգիական մասերը, իսկ գրավիտացիոն դաշտի ազդեցությունը թույլ է: Լարից՝ ֆոնային երկրաչափության կորության շատավղից մեծ հեռավորությունների վրա վակուումային միջիններում գերակշռում են մաքուր դե Սիտտերի երկրաչափությամբ պայմանավորված մասերը: Այդ տիրույթում գրավիտացիոն դաշտի ազդեցությունը տոպոլոգիայով պայմանավորված ներդրումներում կարևոր է և համապատասխան վարքն էապես տարբեր է Մինկովսկու ֆոնի վրա կոսմոլոգիական լարի համեմատ:
7. Ցույց է տրված, որ կոսմոլոգիական ինֆլյացիայի ընթացքում էլեկտրամագնիսական ֆլուկտուացիաների՝ քվանտայինից դասական անցման հետևանքով, հետինֆլացիոն փուլում կոսմոլոգիական լարերը շրջապատված կլինեն մեծամասշտաբ ստոքաստիկ մագնիսական դաշտերով: Այս դաշտերը կարող են հանդես գալ որպես ինֆլյացիայի ընթացքում առաջացած կոսմոլոգիական լարերը, ինչպես նաև համապատասխան ինֆլյացիոն մոդելները բնութագրող առանձնահատկություններ:

СААРЯН НВАРД
НЕКОТОРЫЕ КВАНТОВЫЕ ЭФФЕКТЫ В ГРАВИТАЦИОННЫХ ПОЛЯХ
ЗАКЛЮЧЕНИЕ

Исследовано воздействие гравитационного поля, границ и нетривиальной топологии на квантовые свойства вакуума для скалярного и электромагнитного полей. Вычислены функция Вайтмана, вакуумные средние квадрата поля и тензора энергии-импульса внутри и вне сферы в пространстве с постоянной отрицательной кривизной. Для индуцированных сферой вкладов получены быстро сходящиеся интегральные представления. Воздействие гравитационного поля на вакуумные средние существенно на расстояниях от сферы больших по сравнению с радиусом кривизны пространства. Для заряженного скалярного поля исследованы функция Аадамара и вакуумное среднее плотности тока в плоском пространстве-времени с тороидально компактными пространственными измерениями при наличии плоско-параллельных границ и постоянного калибровочного поля. Вдоль компактных измерений поле удовлетворяет условиям квазипериодичности с произвольными фазами, а на границах наложены граничные условия Робина. Вакуумная плотность тока имеет ненулевые компоненты только вдоль компактных измерений. Получены электромагнитные цилиндрические моды в пространстве де Ситтера при наличии цилиндрической границы. На их основе исследованы вакуумные средние квадрата электрического поля и тензора энергии-импульса. Явно выделены индуцированные границей вклады и рассмотрено их поведение в различных предельных случаях. Исследованы двухточечные функции электромагнитного поля, вакуумные средние квадратов электрического и магнитного полей, а также плотности энергии в окрестности космической струны в пространстве де Ситтера. Показано, что вблизи струны воздействие гравитационного поля на вакуумные средние является слабым, тогда как на расстояниях, больших по сравнению с радиусом кривизны пространства, это воздействие существенно.

1. Для скалярного поля с граничным условием Робина на сфере в пространстве с постоянной отрицательной кривизной явно выделены индуцированные границей вклады в функции Вайтмана, в вакуумных средних квадрата поля и тензора энергии-импульса. В результате, перенормировка вакуумных средних сводится к перенормировке в геометрии без границы. Соответствующие результаты обобщены для пространств со сферическими пузырями и для космологических моделей с отрицательной кривизной. Для значений коэффициента граничного условия, больших некоторого критического значения, скалярный вакуум становится неустойчивым.
2. На расстояниях от сферы, больших по сравнению с радиусом кривизны фонового пространства, индуцированные границей вклады стремятся к нулю быстрее чем в геометрии Минковского. Они убывают по экспоненциальному закону как для массивных, так и для безмассовых полей.
3. Для скалярного поля на фоне с тороидально компактными пространственными измерениями и с плоскими границами, нетривиальные фазы в условиях

квазипериодичности и постоянное калибровочное поле индуцируют вакуумную плотность тока. Она является периодической функцией магнитного потока, охватываемого компактными измерениями, с периодом равным кванту потока.

4. Плотность тока не содержит поверхностных расходимостей и обращается в нуль на границах для условия Дирихле. Нормальная производная плотности тока равна нулю на границах для условий Дирихле и Неймана. В пространстве параметров граничных условий Робина имеется область, где вакуумное состояние становится нестабильным. Условие стабильности зависит от длин компактных измерений и является более слабым, чем в пространстве с тривиальной топологией.
5. Найдены полные системы цилиндрических мод электромагнитного поля внутри и вне цилиндрической поверхности в фоновом пространстве-времени де Ситтера, вычислены вакуумные средние квадрата электрического поля и тензора энергии-импульса. Индуцированный границей вклад в среднее квадрата поля является положительным как внутри, так и вне границы, а соответствующие силы Казимира-Полдера направлены к границе. Вакуумный тензор энергии-импульса, наряду с диагональными компонентами, имеет недиагональную компоненту, которая соответствует потоку энергии в направлении нормали к границе. Поток направлен от границы как во внешней, так и во внутренней областях. Результаты обобщены для граничных условий конфайнмента в квантовой хромодинамике.
6. Для корреляторов электромагнитного поля в окрестности космической струны в пространстве де Ситтера выведены выражения в которых явно выделены индуцированные струной топологические вклады. Благодаря этому, перенормировка локальных вакуумных средних в пределе совпадения сводится к перенормировке в пространстве де Ситтера при отсутствии космической струны. В области вблизи струны, в вакуумных средних квадратов электрического и магнитного полей и плотности энергии доминируют топологические части, а воздействие гравитационного поля является слабым. На расстояниях от струны, больших по сравнению с радиусом кривизны фоновой геометрии, в вакуумных средних доминируют части, обусловленные чистой де Ситтеровской геометрией. В этой области воздействие гравитационного поля на обусловленные топологией вклады является важным и соответствующее поведение существенно отлично по сравнению с космической струной на фоне Минковского.
7. Показано, что вследствие квантово-классического перехода электромагнитных флуктуаций в ходе космологической инфляции, в постинфляционной стадии космические струны окружены стохастическими магнитными полями. Эти поля являются характерными особенностями космических струн, образующихся в ходе инфляции, а также соответствующих инфляционных моделей.